The Coefficient of Variation as a Performance Metric of MIMO Antenna Systems under Arbitrary Handset Orientations

Abbas Al-Wahhamy[1, *], Hussain Al-Rizzo[1], and Nicholas E. Buris[2]

Abstract—The Coefficient of Variation (CoV) is investigated, studied, and proposed as an alternative and important performance metric to describe the effects of handset orientation on the capacity of Multiple-Input-Multiple-Output (MIMO) systems. We combine 3-D simulated radiation patterns of a base station and handset and their associated scattering parameters in two anisotropic propagation environments. The capacity is evaluated as the handset rotates about the X-Y-Z axes using standard Euler's angles. The coefficient of variation is numerically derived by rotating the handset over the Euler angles (φ, θ, ψ) in each direction every 15° about each axis over a full sphere where each rotation involves the creation of numerous instances of the propagation environment depending on the statistical robustness of the results sought. Three antenna array geometries operating at a frequency of 2.45 GHz are examined using two different propagation channel models (TGnB and TGnF) to verify the validity of the proposed approach. The derived results suggest that the proposed CoV is an effective and practical reasonable metric in selecting the best antenna system design, where "best" here refers to the design with the ability to reach the highest throughput of the designs considered.

1. INTRODUCTION

The design of antenna arrays for a handset has a significant impact on the MIMO performance of a mobile device [1–6]. Designing efficient MIMO antennas for mobile terminals is very challenging due to the influence of user orientation [1, 7–12]. The orientation of a handset antenna has a substantial impact on the interaction of the 3-D radiation patterns with the wireless channel in MIMO systems. The handset performance affects the overall network performance; it also affects the total capacity in the network since end-users with non-optimal handsets operate at lower modulation and coding scheme [1–12]. Therefore, industry seeks accurate methods to assess and evaluate the effects of orientation of the handset on the performance in MIMO systems [7].

At the mobile side, the effects of orientation on the performance of MIMO systems have received considerable research attention where the handset is often tested using many different orientation angles [8–14]. In [11], the impact of random handset orientation using Macro-cell and Pico-cell channel models is studied. In [12] and [14], MIMO antenna performance is compared with different polarizations as a function of antenna orientation in terms of capacity. The influence on the throughput performance due to the handset polarization has been presented in [14–18].

A smartphone equipped with a number of sensors which provide information on orientation and rotation can be used to design better handsets and improve network performance. For example, an accelerometer sensor has been used to analyze smartphone orientation and to evaluate smartphone performance [19–21]. The data of the accelerometer sensor were collected using a smartphone application program installed onto several phones. The 3D Cartesian coordinated can be provided using a single accelerometer reading which can be used to describe the phone rotation around the three axes. The

[1] Systems Engineering Department, University of Arkansas at Little Rock, Little Rock, AR, USA. [2] School of Communication and Information Engineering, Shanghai University, Shanghai, China.

effect of orientation and rotation of smartphones on the performance of directional antennas under various propagation environments is reported in [22] by collecting the readings of accelerometer and compass from 11 smartphones users, each one for a week in the field along with network measurements, like signal strength and quality.

Gyroscope sensor is another smartphone sensor used to collect the orientation data from the handset in a real network to evaluate the performance of mobile stations in which the model is based on the three standard angles of the mobile phone [23]. In [21], analysis of orientation and rotation using gyroscope for a phone placement recognition uses a collected dataset from 35 people of 8 different positions. The results are analyzed statistically using mean, standard deviation, root mean square, zero-crossing rate, and absolute value.

Furthermore, performance degradation in a random-LoS environment due to polarization deficiencies is reported in [15] and [24].

It can be seen from the literature survey above that the focus is on evaluating the effects of orientation using simulation [10, 16], or by conducting experimental testing [1, 7, 12], for a specific antenna structure. It should be pointed out that the data collected in previous literature analysis are based on comparing the standard deviation, root mean square, zero-crossing rate, and absolute value. It is not enough to evaluate the handset orientation performance of different mean values. In our study, however, we propose for the first time a single metric, the CoV, to evaluate the performance of cell phones under different orientations. Moreover, designing a handset which is usually used in arbitrary orientation in any environment requires the antenna array to have low peak-to-average performance in terms of the capacity versus orientation. This is because it is desired to have a MIMO antenna array with lower peak performance, but whose capacity remains somewhat independent of the orientation. In other words, it is not desirable to have a product which performs extremely well in some cases and very badly in others.

In this paper, we report on the effects of the orientation of three antenna configurations with different polarizations in two different anisotropic channels. The performance is assessed using a new metric based on CoV in an attempt to deduce the antenna type that provides minimum performance degradation due to antenna rotation. Several antennas operating at 2.45 GHz are considered in this paper using two different propagation environments, and the capacity is simulated at each angle to extract the CoV at a 10 dB Signal-to-Noise Ratio (SNR) at the receiver.

Four antenna types including vertical, cross, and $\pm45°$ slanted dipoles as well as a planar antenna inside a realistic phone model are used in two anisotropic channel models to validate the proposed CoV metric for assessing the performance of a MIMO antenna array under different orientations.

The remainder of this paper is organized as follows. Section 2 presents the formal definition of rotation angles in three dimensions. Section 3 describes the proposed CoV metric, handset configurations, antenna element design, handset phone model, and open-loop capacity. Results and discussions are presented in Section 4. Finally, conclusions are drawn in Section 5.

2. HANDSET ROTATIONS IN THREE DIMENSIONS

An arbitrary three-dimensional rotation can be obtained by three individual rotations around three axes. The orientation of one Cartesian coordinate system with respect to another can be described in terms of three successive rotations around the coordinate axes [25]. For a handset, the Euler rotations are performed about each of the three Cartesian axes.

For example, a handset can be used in several typical positions and orientations: held by one or two hands in "data" or "browsing" modes, lying on a table, normal "talk" mode, in the pocket (horizontal or vertical), etc. Euler defined and popularized three rotations and their specific orders to describe an arbitrary rotation. The first rotation is about the z-axis by an angle φ, the second by an angle θ about the rotated x-axis, and the third rotation by an angle ψ around the rotated y-axis. These three rotations are illustrated in Figure 1.

In this way, all possible antenna orientations in three dimensions can be represented with a triplet of rotation angles. It should be noted that in our simulation models, sweeping is performed overall possible angles with a 15-degree step resulting in 343 rotations of the three Euler's angles as shown in Table 1.
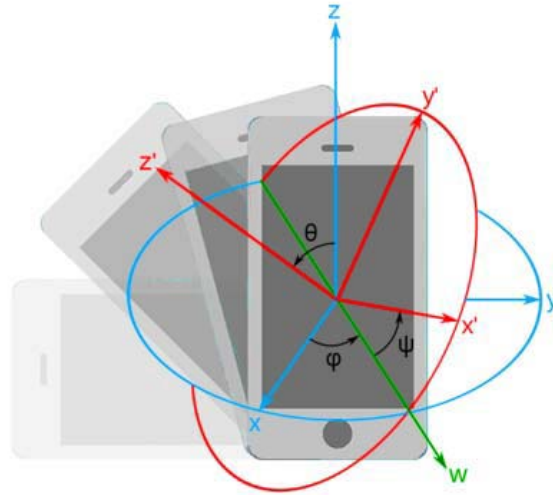
Figure 1. Definitions of Euler's angles.

Table 1. Euler's angles sweeps.

Angle	Initial Value	Step	End Value
φ (°)	0	15	90
θ (°)	0	15	90
ψ (°)	0	15	90

3. COEFFICIENT OF VARIATION

One of the most commonly used statistical measures of variations in scientific and engineering applications is variance and standard deviation. However, when the main purpose is to compare the variation of distributions of a phenomenon with several variables, the standard deviation is not the most appropriate indicator unless all the variables are expressed in the same measurement units and have identical mean values. When these two requirements are not met, the CoV, which is the ratio of standard deviation to the mean [26], is used to describe the amount of variation and can be expressed as:
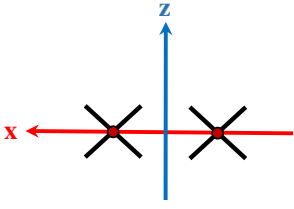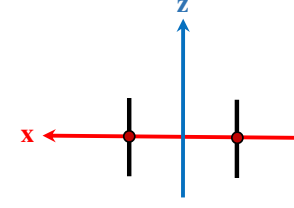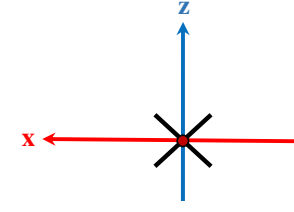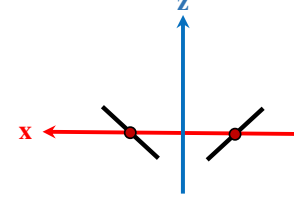
$$\text{CoV} = \frac{\sigma}{\mu} \times 100 \tag{1}$$

where μ and σ are the mean and standard deviation of the variable distribution, respectively. This distribution is taken as the mean capacity evaluated at each of the 343 orientations for a given antenna with SNR = 10 dB. The mean and standard deviation of the mean capacity are computed using the above-mentioned distribution. Based on the discussion in Section 1, in general, it is desired to design for a low CoV.

The variation of the capacity in the data series that represents the 343 samples around the mean is represented by the standard deviation. The performance of an antenna array depends upon the characteristics of the individual radiating elements, geometry, and orientation. Initially, we consider a communication link with a base station that has a 4-port crossed-dipole antenna mounted at a height of 10 m above ground level and three reference 2-port dipole designs configured as vertical-, cross-, and $\pm 45°$ slanted-polarized antennas as shown in Table 2.

Half-wavelength dipole antenna arrays are very popular in many civilian and military applications and have been extensively researched in the past and are still of great interest for personal wireless devices, unmanned devices, automobiles, wireless sensor nodes, MIMO-based handheld, and rooftop-mounted access points of WLAN/Wi-Fi [27–29]. These antennas are designed to work at 2.45 GHz

Table 2. Base station, reference antennas and handset configurations.

Base Station 4-port cross-polarized antenna	
Reference design 1 Two-port vertical-polarized antenna	
Reference design 2 Two-port cross-polarized antenna	
Reference design 3 Two-port slanted ±45° polarized antenna	

(2.4–2.5 GHz ISM band). The distance between non-co-located adjacent dipoles is taken as 60 mm (a little less than $\lambda/2$ at 2.45 GHz) with impedance bandwidth, expressed in terms of the reflection coefficient, $|S_{11}| < -12$ dB, and mutual coupling expressed in terms of $|S_{21}| < -14$ dB at 2.45 GHz. Later, the proposed algorithm is tested using an array of two Inverted-F Antennas (IFAs) which are very popular for handheld devices [30].

The simulation procedure involves two major steps, and the first is using CST Microwave Studio [30]. CST is used to rigorously design and model the antenna arrays at the base station and user equipment. The information extracted from CST which is next exported to the MIMObit software [30] includes the scattering parameters and 3D radiation patterns of the horizontally and vertically polarized components of the far-field electric field vector. The second step is to evaluate the mean capacity of the MIMO system in a given orientation which is evaluated using ten instantiations of the propagation environments in order to achieve a statistically reliable estimates.

We assume that the mean capacity of the MIMO system is evaluated using ten instantiations of the propagation environments. The base station transmits 1 W power equally distributed among the antenna elements. The handset antenna height is 1.5 m above ground level. The distance between the BS and the handset is assumed to be 150 m. The SNR is taken as a healthy 10 dB in all the studies reported in this paper since the relative performance improvement of MIMO systems compared to SISO is higher at low SNRs. IEEE 802.11n TGnB and TGnF propagation channel models [34] are used in the simulations. Table 3 lists the simulation setup parameters.

Table 3. Simulation setup parameters.

Parameter	Value
Carrier Frequency	2.45 GHz
Bandwidth	2.4–2.5 GHz
Propagation Environments	TGnB, TGnF
Base station height	10 m
Handset height	1.5 m
Base-Station antenna polarization	Cross-polarized
Handset antenna polarization	vertical-, cross-, and ±45° slanted-polarized
Antenna element spacing	0.5λ
Base-Station antenna configuration	4-port cross-polarized
Handset antenna configuration	2

MIMObit [31] is used for the rigorous electromagnetic and circuit simulation of the base station antennas and the handset antennas which are both coupled to the channel models to estimate the capacity.

The handset is finally rotated using the aforementioned 343 orientations through rotation around the X-Y-Z axes (Euler angles φ, θ, and ψ, respectively). For each orientation, ten instantiations of the TGnB and TGnF propagation models have been used (3430 different simulations for each curve displaying the capacity versus Euler's angles and propagation model refer to Figures 7 and 9, respectively).

3.1. Reference Antenna Element Design

This paper evaluates the performance of a handset in a MIMO system in terms of CoV using average channel capacity. Three Reference 2-port antenna designs are considered for comparison purposes. Each equipped with two identical dipoles but with different polarizations and spatial separation characteristics as shown in Table 2.

Reference design 1 shows the configuration of two vertical (2V) dipoles, and reference design 2 shows the configuration of two cross-polarized (2X) dipoles which is composes of two slanted ±45° dipoles, while reference design 3 shows the configuration of two slanted ±45° dipoles (2VX).

3.2. Antenna Array inside a Realistic Mobile Phone

In this section, a dual Planar Inverted-F Antenna (PIFA) is used to validate our CoV scheme using a realistic cellular phone model [32]. Variations of PIFAs are popular due to their compact size and ease of manufacturing. Several MIMO PIFA designs for the handset have been recently reported [33–37]. The realistic handset study enables the evaluation of the performance of the antenna array taking into consideration of the coupling effects due to nearby objects such as camera, battery, as well as housing and screen as compared to the standalone reference antennas analyzed in Section 3.1. The geometry of the dual-band PIFA shown in Figure 2 is designed to operate at the Wi-Fi bands of 2.4 GHz and 5 GHz. CST Microwave Studio (CST MWS) which is based on the FIT method of Computer Simulation Technology is used to simulate the scattering matrix and 3D patterns. The body of the mobile phone is modeled using plastic with dimensions 136 mm × 69 mm × 8 mm. The Liquid Crystal Display (LCD), dimensions 112 mm × 64 mm × 0.35 mm, has been added.

Figure 2 indicates the cellphone antenna model within the body structure. The dimensions of the handset components are similar to those encountered in the market. The Wi-Fi antennas seen in Figure 2 are placed at the upper sides of the phone.
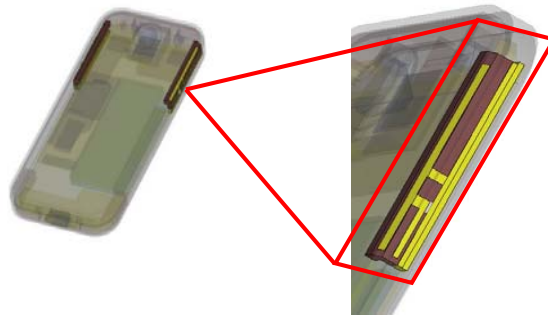
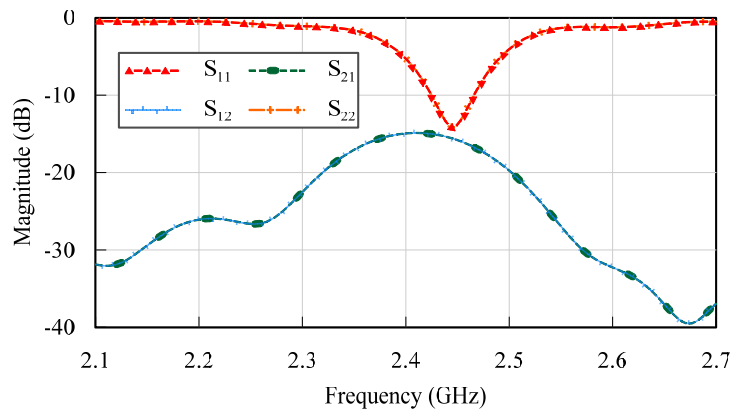**Figure 2.** PIFA antennas placement in a full realistic phone model.

Figure 3. Return loss characteristics of the PIFA.

The distance between the two antenna ports is 63.9 mm. Figure 3 shows S_{11} and S_{21} of the PIFA antennas. From Figure 3, it can be seen that the 10 dB impedance bandwidth is 30 MHz from 2.43 to 2.46 GHz, and the port isolation is reasonable at $S_{21} < -10$ dB over the bandwidth.

The simulated 3D radiation patterns at 2.45 GHz when one antenna is excited and the other terminated by a matched load are shown in Figure 4.

The CoV is numerically evaluated in this case by rotating the phone using 8125 orientation increments around the X-Y-Z axes (Euler angles φ, θ, and ψ, respectively) using a full sphere rotation
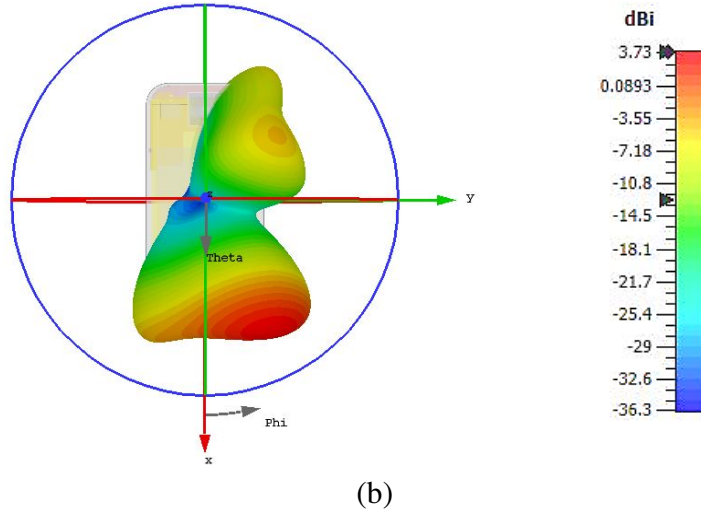

(a)

(b)
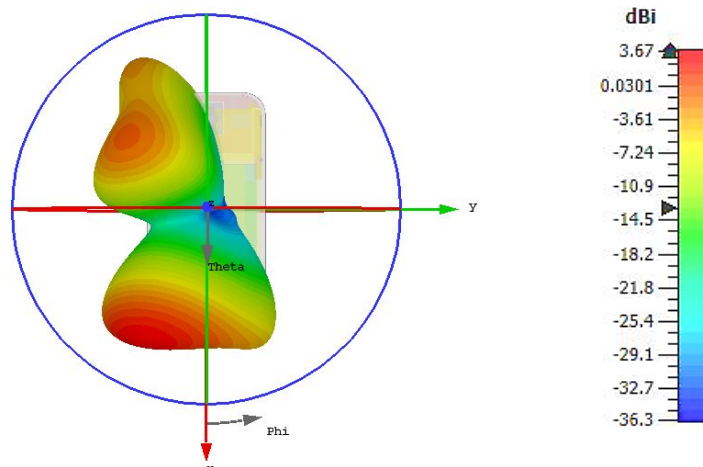
Figure 4. Simulated 3D gain pattern at 2.45 GHz. (a) Port-1. (b) Port-2.

as shown in Table 4 due to the asymmetric 3D patterns. For each orientation, ten instantiations of the TGnB and TGnF propagation models have been used (81250 different simulations for each curve displaying the capacity versus Euler's angles and propagation model, refer to Figure 11).

Table 4. Euler's angles sweeps for a full-phone model.

Angle	Initial Value	Step	End Value
φ (°)	0	15	360
θ (°)	0	15	180
ψ (°)	0	15	360

3.3. Open-Loop Capacity

The open-loop MIMO capacity normalized by the transmission bandwidth, which is refer to as the link efficiency, is used throughout the paper to assess the performance of the MIMO system where a set of orthogonal signals is transmitted using the same available power for each and is defined as [38]:

$$C_{\text{MIMO}} = \log_2 \left[\det \left(\bar{\bar{I}} + \frac{P_T}{N_T P_n} \bar{\bar{H}}(f_o) \cdot \bar{\bar{H}}^T(f_o) \right) \right] \qquad (2)$$

where $\bar{\bar{I}}$ is the identity matrix, $\bar{\bar{H}}(f_o)$ the channel matrix that contains the effects of the antennas, their terminations, channel P_T the total power available at the transmitter, $\bar{\bar{H}}^T(f_o)$ the Hermitian of $\bar{\bar{H}}(f_o)$, N_T the number of transmitting antennas, and P_n the average noise power per receiving antenna. Results are derived using the open-loop capacity formula where the signals supplied from the voltage sources of each transmitter are orthogonal and have equal "available" power.

4. RESULTS AND DISCUSSION

The TGnB and TGnF propagation characteristics are presented in Figures 5(a) and 6(a), respectively, as 3D graphs of the transmitted Angle of Departure (AoD) and received Angle of Arrivals (AoA) for a given handset orientation. The delay ("tap") plots for the TGnB and TGnF propagation scenarios are also shown in Figures 5(b) and 6(b), respectively.
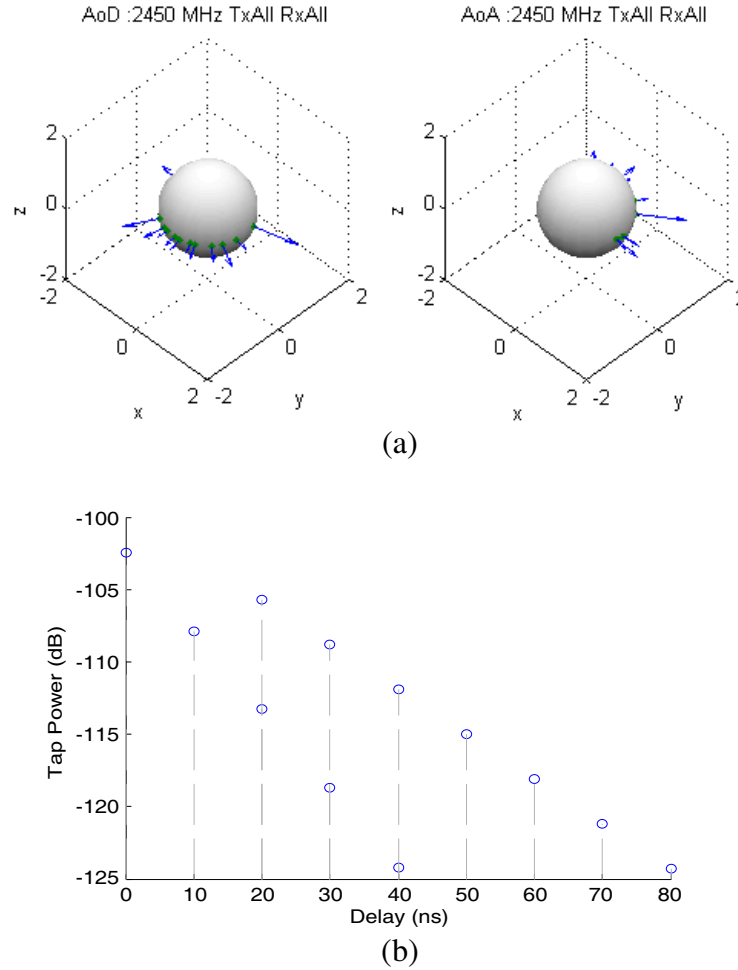
Figure 5. TGnB propagation characteristics. (a) Propagation environment plot. (b) Tap delay plot for TGnB model.

In order to define a metric for the effects of handset orientation on the channel capacity, the link efficiency which is extracted from the 50% point of the CDF curve of the link efficiency for each instantiation of a given orientation angle considered in the simulation is evaluated in each direction every 15° over a full sphere. The same calculations are repeated in non-line-of-sight (NLOS) environments using two models (TGnB and TGnF). Figures 7, 9, and 11 present the average capacity traces for each antenna configuration at 10 dB SNR for the two propagation channel models. The major contribution of this paper is to answer the question that may arise: how to figure out which antenna system is the best from these graphs?

As can be seen from Table 5 and Table 6, the mean and standard deviation for the data presented in Figures 7, 9, and 11 are (3.275, 0.836), (3.519, 0.549), (4.066, 0.585), and (5.487, 0.635), respectively for TGnB while for TGnB are (1.902, 0.562), (1.528, 0.289), (2.274, 0.391), and (5.699, 0.694), respectively. It is not reasonable to compare the performance of these four cases due to the difference in mean and standard deviations (the CoV reveals that a lower standard deviation alone does not imply less variable data). However, the CoV is unitless and can deliver information which the standard deviation cannot, has been proven as a meaningful measure in many disciplines [39–42], and can be easily obtained from the data presented in Figures 7, 9, and 11 to compare the performance of the four antenna configurations unlike using the standard deviation alone as the four configurations have different means [26].

Figures 8, 10, and 12 show the mean capacity over the entire sweep of Euler's angles for the TGnB and TGnF channel models, respectively. Box and Whisker plots are used to visualize the variation due

Table 5. Coefficient of variation for TGnB model.

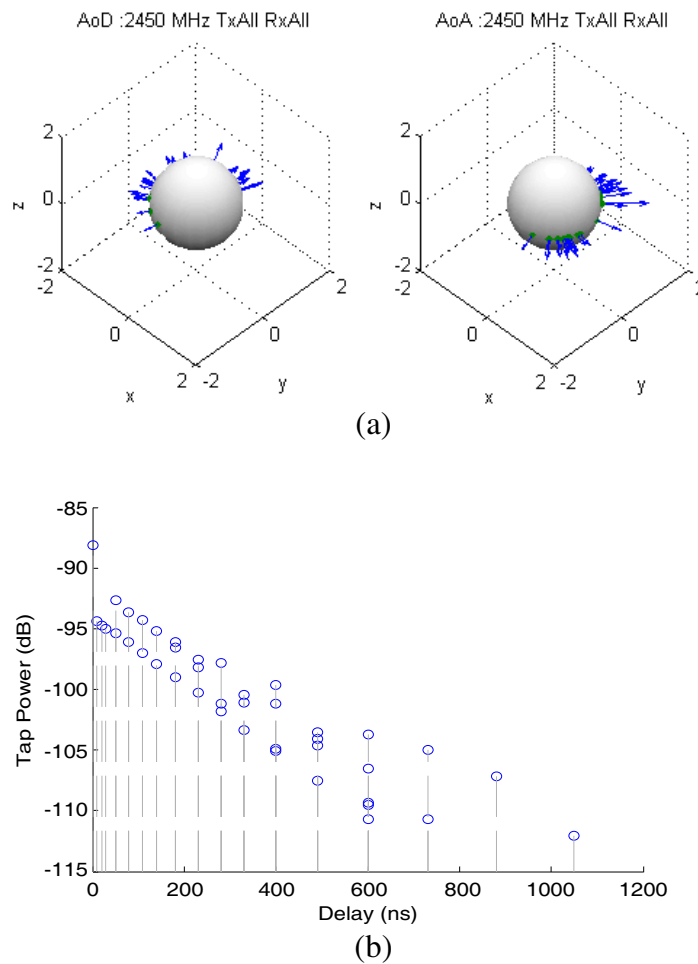| Handset Antenna Configuration Type	Coefficient of Variation (Unitless)	Standard Deviation (bps/Hz)	Mean (bps/Hz)
Reference design 1 (2V)	25.52	0.836	3.275
Reference design 2 (2X)	15.48	0.549	3.519
Reference design 3 (2VX)	14.39	0.585	4.066
Full-Phone Model	11.57	0.635	5.487

(a)

(b)

Figure 6. TGnF propagation characteristics. (a) Propagation environment plot. (b) Tap delay plot for TGnF model.

to reference designs and the handset orientation. Box and Whisker plot is a convenient way of visually displaying the data distribution through their quartiles and powerful graphical technique for comparing two or more variation distributions. The box represents the central mass of the variation, and the ends of the box represent the upper and lower quartiles. The two lines extending from the boxes are called whiskers, which are indicated variability outside the upper and lower quartiles. In this paper, the ends of the whiskers represent the min and max values of the quantity plotted. The single data points that are in-line with whiskers are called outliers which is useful for showing potential unusual observations in the data. From the three figures, it can be noticed that the 2VX is better than 2X

Table 6. Coefficient of variation for TGnF model.

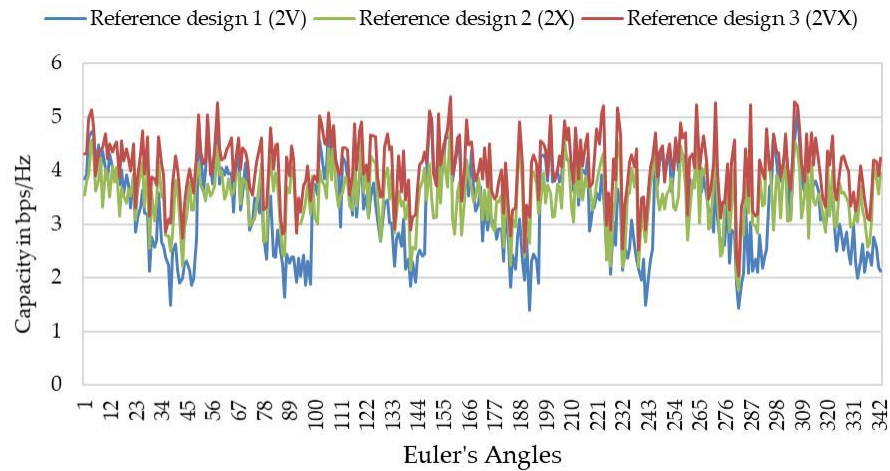| Handset Antenna Configuration Type	Coefficient of Variation (Unitless)	Standard Deviation (bps/Hz)	Mean (bps/Hz)
Reference design 1 (2V)	29.53	0.562	1.902
Reference design 2 (2X)	18.93	0.289	1.528
Reference design 3 (2VX)	17.18	0.391	2.274
Full-Phone Model	12.18	0.694	5.699

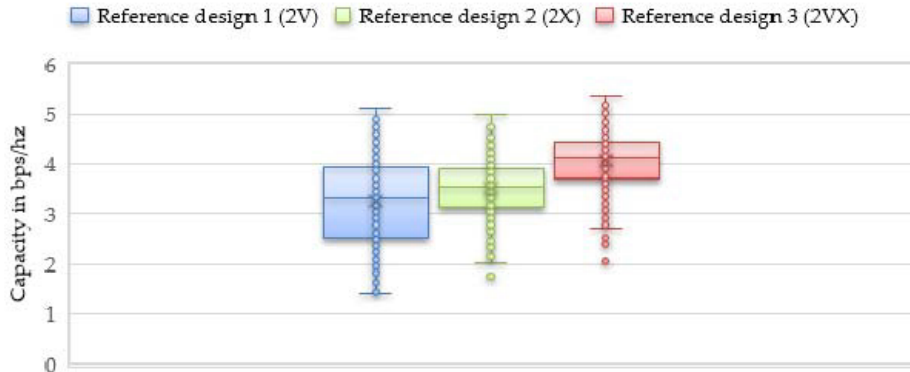**Figure 7.** The capacity in bps/Hz vs. Euler's angles plot for TGnB propagation model.

Figure 8. Box and Whisker plot to represent CoV for TGnB model.

and 2V because it has a larger minimum value and the highest maximum value. Moreover, the 2VX has minimum variation around the highest mean value. Meanwhile, the CoV for the realistic phone model shows the lowest CoV value due to the asymmetric 3D patterns with their boresights pointing in opposite directions, unlike the omnidirectional standalone antennas. Moreover, the omnidirectional antennas propagate signals equally in all directions in the horizontal plane but have limited range on the vertical plane.

Table 5 and Table 6 show the CoV, standard deviation, and mean values for each handset configuration in TGnB and TGnF propagation channels, respectively. A low value of CoV indicates lower fluctuations in channel capacity around the maximum mean capacity due to handset orientation.
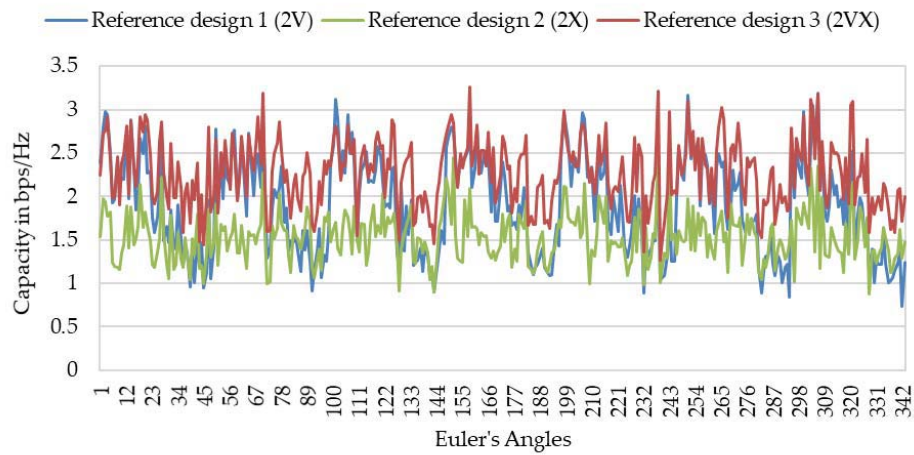
Figure 9. The capacity in bps/Hz vs. Euler's angles plot for TGnF propagation model.
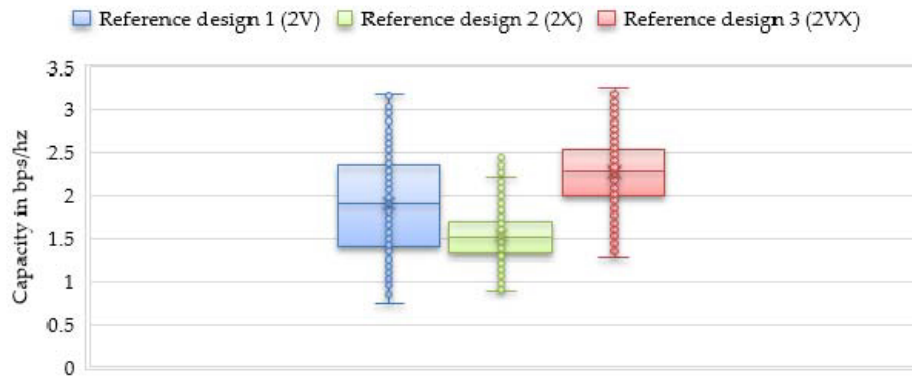

Figure 10. Box and Whisker plot to represent CoV for TGnF model.
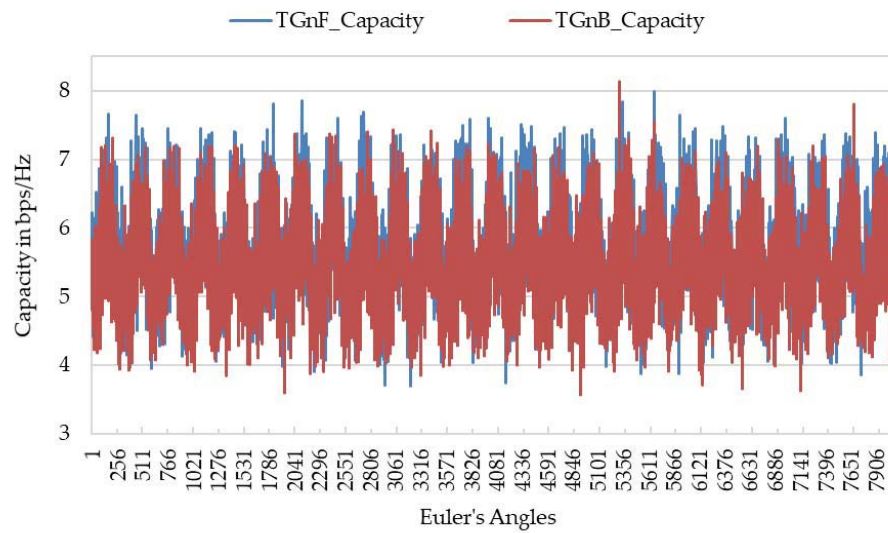

Figure 11. The capacity in bps/Hz vs. Euler's angles plot for full-phone model at TGnB and TGnF.
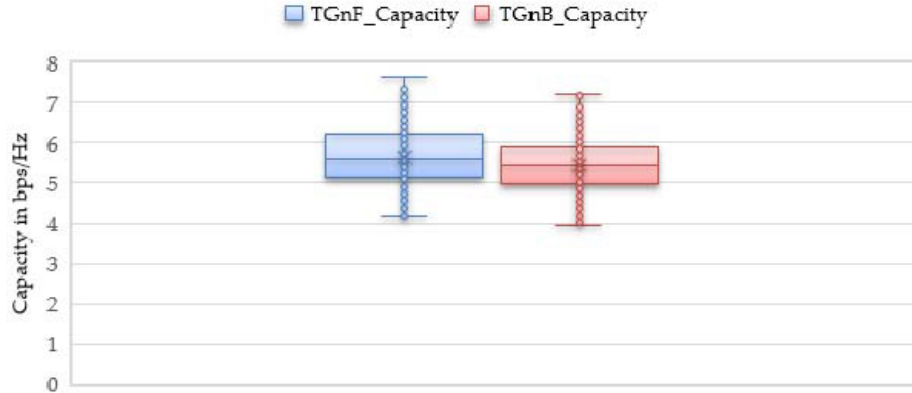
Figure 12. Box and Whisker plot (phone in TGnB and TGnF environments).

However, the standard deviation alone will not assist the designer to judge which handset antenna configuration behaves better than others. In the first reference design 2V, the CoV is higher than the other three configurations which means a high peak-to-average performance in the mean capacity versus orientation which is not preferred when designing a handset that is typically used in arbitrary orientations. Secondly, in reference design 2X, the CoV is lower than the that of 2V, leading to a better design. For the third handset configuration, 2VX, the CoV is the lower than the other two reference designs, 2V and 2X. Finally, the full-phone model shows the lowest CoV value among all configurations, implying that the capacity is the least dependent on the orientation, in relative terms. Hence, the full-phone model provides better antenna system design than the reference designs considered in this paper. This is an indication that the geometrical complexity of real handsets actually renders the product better matched to the unavoidably complex propagation environments. At the limit of the simplest scenario, i.e., 1-port antenna in a Line of Sight propagation environment, the CoV would be very high as the received power can go from its maximum value to zero by a simple 90-degree rotation. The exact value would, of course, depend on the directivity of the antenna. Likewise, we expect that using a little more complex reference designs, e.g., simple antennas on unpopulated printed circuit boards, will likely result in a more biased design than the full-phone model, and consequently, it will result in a higher CoV than that of the full-phone model in complex propagation environments.

5. CONCLUSIONS

In this paper, we have presented a method for evaluating the open loop capacity performance of the handset with arbitrary orientation in MIMO systems using CoV. The method has been demonstrated using three reference design antenna systems and a realistic full-phone model. Two propagation channel models at a fixed SNR at the handset have been used for the simulation studies. The statistical robustness of the results provided by the CoV method can be adjusted by changing the sweep angle step and the number of channel instantiations.

The variation in MIMO performance due to the handset orientation has great influence on product designs. CoV can be a beneficial measure when determining if a given antenna array is a good fit for a specific task. Additional studies and corroboration by other researchers could turn the CoV to a more meaningful MIMO antenna system performance metric than some of those used currently. For example, it should be appreciated that the CoV of the capacity is more relevant than the Envelope Correlation Coefficient (ECC) as the latter cannot be directly associated with the achievable capacity

REFERENCES

1. Lehne, P. H., K. Mahmood, A. A. Glazunov, et al., "Measuring user-induced randomness to evaluate smart phone performance in real environments," *2015 9th European Conference on Antennas and Propagation (EuCAP)*, 1–5, Apr. 2015.

2. Al-Wahhamy, A., N. E. Buris, H. M. Al-Rizzo, and S. Yahya, "An efficient paradigm for evaluating the channel capacity of closed-loop massive MIMO systems," *Progress In Electromagnetics Research C*, Vol. 98, 1–16, 2020.

3. Al-Wahhamy, A., H. Al-Rizzo, and N. E. Buris, "Efficient evaluation of massive MIMO channel capacity," *IEEE Syst. J.*, Vol. 14, No. 1, 614–620, Mar. 2020, doi: 10.1109/JSYST.2019.2900006.

4. Isaac, A. A., H. Al-Rizzo, S. Yahya, A. Al-Wahhamy, and S. Abushamleh, "Decoupling of two closely-spaced planar monopole antennas using two novel printed-circuit structures," *Microw. Opt. Technol. Lett.*, Vol. 60, No. 12, 2954–2963, Dec. 2018, doi: 10.1002/mop.31405.

5. Abbosh, A., H. Al-Rizzo, S. Yahya, and A. Al-Wahhamy, "Decoupling and MIMO performance of two planar monopole antennas with protruded strips," *Microw. Opt. Technol. Lett.*, Vol. 60, No. 11, 2712–2718, Nov. 2018, doi: 10.1002/mop.31487.

6. Isaac, A. A., H. Al-Rizzo, S. Yahya, A. Al-Wahhamy, and S. Z. Tariq, "Miniaturised MIMO antenna array of two vertical monopoles embedded inside a planar decoupling network for the 2.4 GHz ISM band," *IET Microwaves, Antennas Propag.*, Vol. 14, No. 1, 132–140, Jan. 2020, doi: 10.1049/iet-map.2018.5069.

7. Soltani, M. D., A. A. Purwita, Z. Zeng, H. Haas, and M. Safari, "Modeling the random orientation of mobile devices: Measurement, analysis and LiFi use case," *IEEE Trans. Commun.*, Vol. 67, No. 3, 2157–2172, Mar. 2019, doi: 10.1109/TCOMM.2018.2882213.

8. Soltani, M. D., H. Kazemi, M. Safari, and H. Haas, "Handover modeling for indoor Li-Fi cellular networks: The effects of receiver mobility and rotation," *2017 IEEE Wireless Communications and Networking Conference (WCNC)*, 1–6, Mar. 2017, doi: 10.1109/WCNC.2017.7925676.

9. Purwita, A. A., M. Dehghani Soltani, M. Safari, and H. Haas, "Impact of terminal orientation on performance in LiFi systems," *2018 IEEE Wireless Communications and Networking Conference (WCNC)*, 1–6, Apr. 2018, doi: 10.1109/WCNC.2018.8377334.

10. Almesaeed, R., A. S. Ameen, A. Doufexi, and A. R. Nix, "Exploiting the elevation dimension of MIMO system for boosting handset capacity," *2015 IEEE International Conference on Communication Workshop (ICCW)*, 1281–1285, Jun. 2015, doi: 10.1109/ICCW.2015.7247354.

11. Mellios, E., Z. Mansor, G. S. Hilton, A. R. Nix, and J. P. McGeehan, "Impact of antenna pattern and handset rotation on macro-cell and pico-cell propagation in heterogeneous LTE networks," *Proceedings of the 2012 IEEE International Symposium on Antennas and Propagation*, 1–2, Jul. 2012, doi: 10.1109/APS.2012.6348849.

12. Harrysson, F., J. Medbo, A. F. Molisch, A. J. Johansson, and F. Tufvesson, "Efficient experimental evaluation of a MIMO handset with user influence," *IEEE Trans. Wirel. Commun.*, Vol. 9, No. 2, 853–863, Feb. 2010, doi: 10.1109/TWC.2010.02.090588.

13. Buris, N. E., M. Abdul-Gaffoor, and E. Krenz, "Capacity based MIMO antenna design," *2017 IEEE International Symposium on Antennas and Propagation & USNC/URSI National Radio Science Meeting*, 1695–1696, Jul. 2017, doi: 10.1109/APUSNCURSINRSM.2017.8072890.

14. Dao, M.-T., V.-A. Nguyen, Y.-T. Im, S.-O. Park, and G. Yoon, "3D polarized channel modeling and performance comparison of MIMO antenna configurations with different polarizations," *IEEE Trans. Antennas Propag.*, Vol. 59, No. 7, 2672–2682, Jul. 2011, doi: 10.1109/TAP.2011.2152319.

15. Razavi, A., A. A. Glazunov, P. S. Kildal, and J. Yang, "Characterizing polarization-MIMO antennas in Random-LOS propagation channels," *IEEE Access*, 2016, doi: 10.1109/ACCESS.2016.2637443.

16. Razavi, A. and A. A. Glazunov, "Probability of detection functions of polarization-MIMO systems in Random-LOS," *IEEE Access*, 2017, doi: 10.1109/ACCESS.2017.2769804.

17. Soltani, M. D., A. A. Purwita, Z. Zeng, H. Haas, and M. Safari, "Modeling the random orientation of mobile devices: Measurement, analysis and LiFi use case," *IEEE Trans. Commun.*, 2019, doi: 10.1109/TCOMM.2018.2882213.

18. Watthanapak, W., A. Namahoot, and S. Chalermwisutkul, "Effects of reader antenna orientation on received signal strength of UHF RFID tags for handheld reader localization," *2019 Research, Invention, and Innovation Congress (RI2C)*, 1–4, Dec. 2019, doi: 10.1109/RI2C48728.2019.8999931.

19. Lehne, P. H., A. A. Glazunov, K. Mahmood, and P.-S. Kildal, "Analyzing smart phones' 3D accelerometer measurements to identify typical usage positions in voice mode," *2016 10th European Conference on Antennas and Propagation (EuCAP)*, 1–5, Apr. 2016, doi: 10.1109/EuCAP.2016.7481895.

20. Blum, J. R., D. G. Greencorn, and J. R. Cooperstock, *Smartphone Sensor Reliability for Augmented Reality Applications*, 127–138, Springer, Berlin, Heidelberg, 2013.

21. Incel, O., "Analysis of movement, orientation and rotation-based sensing for phone placement recognition," *Sensors*, Vol. 15, No. 10, 25474–25506, Oct. 2015, doi: 10.3390/s151025474.

22. Amiri Sani, A., L. Zhong, and A. Sabharwal, "Directional antenna diversity for mobile devices," *Proceedings of the Sixteenth Annual International Conference on Mobile Computing and Networking — MobiCom'10*, 221, 2010, doi: 10.1145/1859995.1860021.

23. Dehghani Soltani, M., X. Wu, M. Safari, and H. Haas, "Access point selection in Li-Fi cellular networks with arbitrary receiver orientation," *2016 IEEE 27th Annual International Symposium on Personal, Indoor, and Mobile Radio Communications (PIMRC)*, 1–6, Sep. 2016, doi: 10.1109/PIMRC.2016.7794890.

24. Razavi, A., A. A. Glazunov, P. Kildal, and J. Yang, "Investigation of polarization deficiencies in SIMO systems in Random-LOS propagation channels," *2015 International Symposium on Antennas and Propagation (ISAP)*, No. 1, 1–3, 2015.

25. Jazar, R. N., *Theory of Applied Robotics*, Springer, Boston, MA, USA, 2007.

26. Brown, C. E., "Coefficient of variation," *Applied Multivariate Statistics in Geohydrology and Related Sciences*, 155–157, Springer Berlin Heidelberg, Berlin, Heidelberg, 1998.

27. Chen, Z. N., *Antennas for Portable Devices*, John Wiley & Sons, Ltd, Chichester, UK, 2007.

28. Rabinovich, V., N. Alexandrov, and B. Alkhateeb, *Automotive Antenna Design and Applications*, CRC Press, 2017.

29. Liang, Z. X., et al., "Improved hybrid leapfrog ADI-FDTD method for simulating near-field coupling effects among multiple thin wire monopole antennas on a complex platform," *IEEE Trans. Electromagn. Compat.*, 2017, doi: 10.1109/TEMC.2016.2632129.

30. Zhang, Z., *Antenna Design for Mobile Devices*, 2nd Edition, John Wiley & Sons (Asia) Pte Ltd, Singapore, 2017.

31. NEBENS, "MIMObit," http://www.nebens.com, 2018.

32. CST MICROWAVE STUDIO https://www.cst.com, "CST MICROWAVE STUDIO," 2018.

33. Singh, H. S., G. K. Pandey, P. K. Bharti, and M. K. Meshram, "A compact dual band MIMO/diversity antenna for WLAN applications," *2013 Students Conference on Engineering and Systems (SCES)*, 1–5, Apr. 2013, doi: 10.1109/SCES.2013.6547496.

34. Biswal, S. P. and S. Das, "Two-element printed PIFA-MIMO antenna system for WiMAX and WLAN applications," *IET Microwaves, Antennas Propag.*, Vol. 12, No. 14, 2262–2270, Nov. 2018, doi: 10.1049/iet-map.2018.5271.

35. Biswal, S. P. and S. Das, "A dual band MIMO PIFA for WLAN application," *2017 USNC-URSI Radio Science Meeting (Joint with AP-S Symposium)*, 121–122, Jul. 2017, doi: 10.1109/USNC-URSI.2017.8074927.

36. Chattha, H. T., M. Nasir, Q. H. Abbasi, Y. Huang, and S. S. AlJa'afreh, "Compact low-profile dual-port single wideband planar inverted-F MIMO antenna," *IEEE Antennas Wirel. Propag. Lett.*, Vol. 12, 1673–1675, 2013, doi: 10.1109/LAWP.2013.2293765.

37. Singh, A., S. K. Dash, and V. R. Gupta, "Dual feed planar inverted-F antenna for MIMO application," *2017 Innovations in Power and Advanced Computing Technologies (i-PACT)*, 1–4, Apr. 2017, doi: 10.1109/IPACT.2017.8245108.

38. Al-Wahhamy, A., H. Al-Rizzo, and N. E. Buris, "On the modeling of antenna arrays for massive MIMO systems," *2018 IEEE International Symposium on Antennas and Propagation & USNC/URSI National Radio Science Meeting*, 1565–1566, Jul. 2018, doi: 10.1109/APUSNCURSINRSM.2018.8608402.

39. Estrada, J. H., E. A. Cano-Plata, C. Younes-Velosa, and C. L. Cortés, "Entropy and coefficient of variation (CV) as tools for assessing power quality," *Ing. e Investig.*, 2011.

40. Krishnamoorthy, K., *Handbook of Statistical Distributions with Applications*, Chapman and Hall/CRC, 2016.

41. Sammarco, P. W., A. Winter, and J. C. Stewart, "Coefficient of variation of sea surface temperature (SST) as an indicator of coral bleaching," *Mar. Biol.*, Vol. 149, No. 6, 1337–1344, Sep. 2006, doi: 10.1007/s00227-006-0318-0.

42. Shechtman, O., *The Coefficient of Variation as an Index of Measurement Reliability*, 39–49, Springer, 2013.